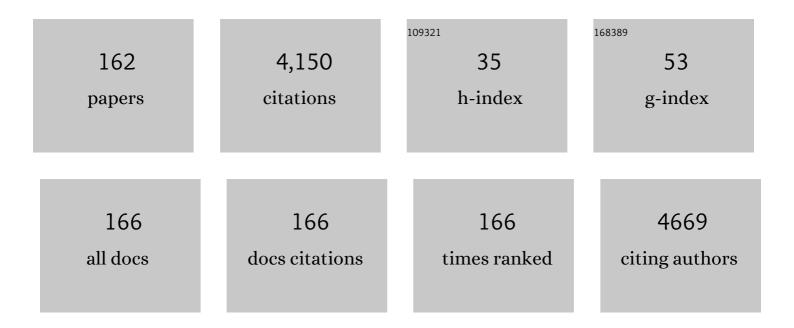
List of Publications by Year in descending order

Source: https://exaly.com/author-pdf/3064357/publications.pdf Version: 2024-02-01



#	Article	IF	CITATIONS
1	Engineering the novel MoSe2-Mo2C hybrid nanoarray electrodes for energy storage and water splitting applications. Applied Catalysis B: Environmental, 2020, 264, 118531.	20.2	136
2	Improved Hydrogen Evolution Reaction Performance using MoS ₂ –WS ₂ Heterostructures by Physicochemical Process. ACS Sustainable Chemistry and Engineering, 2018, 6, 8400-8409.	6.7	111
3	Methane as an effective hydrogen source for single-layer graphene synthesis on Cu foil by plasma enhanced chemical vapor deposition. Nanoscale, 2013, 5, 1221.	5.6	104
4	Large-area, continuous and high electrical performances of bilayer to few layers MoS2 fabricated by RF sputtering via post-deposition annealing method. Scientific Reports, 2016, 6, 30791.	3.3	104
5	Graphene synthesis on Fe foil using thermal CVD. Current Applied Physics, 2011, 11, S81-S85.	2.4	99
6	Direct synthesis of thickness-tunable MoS2 quantum dot thin layers: Optical, structural and electrical properties and their application to hydrogen evolution. Nano Energy, 2017, 35, 101-114.	16.0	99
7	One-pot facile methodology to synthesize MoS2-graphene hybrid nanocomposites for supercapacitors with improved electrochemical capacitance. Composites Part B: Engineering, 2019, 161, 555-563.	12.0	85
8	Fabrication of MoS2/WSe2 heterostructures as electrocatalyst for enhanced hydrogen evolution reaction. Applied Surface Science, 2019, 480, 611-620.	6.1	82
9	Influence of an Al2O3 interlayer in a directly grown graphene-silicon Schottky junction solar cell. Carbon, 2018, 132, 157-164.	10.3	78
10	n-MoS ₂ /p-Si Solar Cells with Al ₂ O ₃ Passivation for Enhanced Photogeneration. ACS Applied Materials & Interfaces, 2016, 8, 29383-29390.	8.0	77
11	Synthesis and characterization of large-area and continuous MoS ₂ atomic layers by RF magnetron sputtering. Nanoscale, 2016, 8, 4340-4347.	5.6	74
12	Hybrid Design Using Carbon Nanotubes Decorated with Mo ₂ C and W ₂ C Nanoparticles for Supercapacitors and Hydrogen Evolution Reactions. ACS Sustainable Chemistry and Engineering, 2020, 8, 12248-12259.	6.7	73
13	Engineering MoSe ₂ /WS ₂ Hybrids to Replace the Scarce Platinum Electrode for Hydrogen Evolution Reactions and Dye-Sensitized Solar Cells. ACS Applied Materials & Interfaces, 2021, 13, 5061-5072.	8.0	69
14	Large area growth of MoTe2 films as high performance counter electrodes for dye-sensitized solar cells. Scientific Reports, 2018, 8, 29.	3.3	68
15	Temperature-Dependent and Gate-Tunable Rectification in a Black Phosphorus/WS ₂ van der Waals Heterojunction Diode. ACS Applied Materials & Interfaces, 2018, 10, 13150-13157.	8.0	61
16	Reversible transition of volatile to non-volatile resistive switching and compliance current-dependent multistate switching in IGZO/MnO RRAM devices. Applied Physics Letters, 2019, 114, .	3.3	60
17	Facile preparation of molybdenum carbide (Mo2C) nanoparticles and its effective utilization in electrochemical sensing of folic acid via imprinting. Biosensors and Bioelectronics, 2019, 140, 111330.	10.1	59
18	Design of Basal Plane Edges in Metal-Doped Nanostripes-Structured MoSe ₂ Atomic Layers To Enhance Hydrogen Evolution Reaction Activity. ACS Sustainable Chemistry and Engineering, 2019, 7, 458-469.	6.7	58

#	Article	IF	CITATIONS
19	Implementation of both high-hole and electron mobility in strained Si/strained Si _{1-y} Ge _y on relaxed Si _{1-x} Ge _x (x <y) substrate.<br="" virtual="">IEEE Electron Device Letters, 2003, 24, 460-462.</y)>	3.9	57
20	Design of WSe ₂ /MoS ₂ Heterostructures as the Counter Electrode to Replace Pt for Dye-Sensitized Solar Cell. ACS Sustainable Chemistry and Engineering, 2019, 7, 13195-13205.	6.7	57
21	Engineering the active sites tuned MoS2 nanoarray structures by transition metal doping for hydrogen evolution and supercapacitor applications. Journal of Alloys and Compounds, 2022, 893, 162271.	5.5	57
22	CuS/WS2 and CuS/MoS2 heterostructures for high performance counter electrodes in dye-sensitized solar cells. Solar Energy, 2018, 171, 122-129.	6.1	50
23	Engineering MoTe2 and Janus SeMoTe nanosheet structures: First-principles roadmap and practical uses in hydrogen evolution reactions and symmetric supercapacitors. Nano Energy, 2021, 87, 106161.	16.0	50
24	Local conductance measurement of graphene layer using conductive atomic force microscopy. Journal of Applied Physics, 2011, 110, .	2.5	49
25	MoS2@X2C (XÂ=ÂMo or W) hybrids for enhanced supercapacitor and hydrogen evolution performances. Chemical Engineering Journal, 2021, 421, 127843.	12.7	49
26	Catalytic decontamination of organic/inorganic pollutants in water and green H2 generation using nanoporous SnS2 micro-flower structured film. Journal of Hazardous Materials, 2021, 417, 126105.	12.4	48
27	Facile and cost-effective methodology to fabricate MoS 2 counter electrode for efficient dye-sensitized solar cells. Dyes and Pigments, 2018, 151, 7-14.	3.7	47
28	Unveiling the Redox Electrochemistry of MOFâ€Derived fccâ€NiCo@GC Polyhedron as an Advanced Electrode Material for Boosting Specific Energy of the Supercapattery. Small, 2022, 18, e2107284.	10.0	43
29	1D-CoSe ₂ nanoarray: a designed structure for efficient hydrogen evolution and symmetric supercapacitor characteristics. Dalton Transactions, 2020, 49, 14191-14200.	3.3	42
30	Physical and electrical properties of graphene grown under different hydrogen flow in low pressure chemical vapor deposition. Nanoscale Research Letters, 2014, 9, 546.	5.7	39
31	Facile method to synthesis hybrid phase 1T@2H MoSe2 nanostructures for rechargeable lithium ion batteries. Journal of Electroanalytical Chemistry, 2019, 833, 333-339.	3.8	39
32	One-Pot Synthesis of W2C/WS2 Hybrid Nanostructures for Improved Hydrogen Evolution Reactions and Supercapacitors. Nanomaterials, 2020, 10, 1597.	4.1	39
33	Growth of Fewâ€Layer Graphene on a Thin Cobalt Film on a Si/SiO ₂ Substrate. Chemical Vapor Deposition, 2011, 17, 9-14.	1.3	38
34	Asymmetric electrode incorporated 2D GeSe for self-biased and efficient photodetection. Scientific Reports, 2020, 10, 9374.	3.3	38
35	Ultrasonically derived WSe2 nanostructure embedded MXene hybrid composites for supercapacitors and hydrogen evolution reactions. Renewable Energy, 2022, 185, 585-597.	8.9	38
36	Induced Superaerophobicity onto a Non-superaerophobic Catalytic Surface for Enhanced Hydrogen Evolution Reaction. ACS Applied Materials & Interfaces, 2017, 9, 43674-43680.	8.0	37

#	Article	IF	CITATIONS
37	Synthesis of Mo2C and W2C Nanoparticle Electrocatalysts for the Efficient Hydrogen Evolution Reaction in Alkali and Acid Electrolytes. Frontiers in Chemistry, 2019, 7, 716.	3.6	37
38	Deep Trench Isolation for Crosstalk Suppression in Active Pixel Sensors with 1.7 µm Pixel Pitch. Japanese Journal of Applied Physics, 2007, 46, 2454-2457.	1.5	35
39	Nanoscale investigation of charge transport at the grain boundaries and wrinkles in graphene film. Nanotechnology, 2012, 23, 285705.	2.6	34
40	Effect of Annealing in Ar/H ₂ Environment on Chemical Vapor Deposition-Grown Graphene Transferred With Poly (Methyl Methacrylate). IEEE Nanotechnology Magazine, 2015, 14, 70-74.	2.0	34
41	WS2/CoSe2 heterostructure: A designed structure as catalysts for enhanced hydrogen evolution performance. Journal of Industrial and Engineering Chemistry, 2018, 65, 167-174.	5.8	34
42	NIR self-powered photodetection and gate tunable rectification behavior in 2D GeSe/MoSe2 heterojunction diode. Scientific Reports, 2021, 11, 3688.	3.3	34
43	Bimetallic Cu/Fe MOF-Based Nanosheet Film via Binder-Free Drop-Casting Route: A Highly Efficient Urea-Electrolysis Catalyst. Nanomaterials, 2022, 12, 1916.	4.1	33
44	Sputtering and sulfurization-combined synthesis of a transparent WS ₂ counter electrode and its application to dye-sensitized solar cells. RSC Advances, 2015, 5, 103567-103572.	3.6	32
45	Growth of a WSe 2 /W counter electrode by sputtering and selenization annealing for high-efficiency dye-sensitized solar cells. Applied Surface Science, 2017, 406, 84-90.	6.1	32
46	Fabrication of MoSe2 decorated three-dimensional graphene composites structure as a highly stable electrocatalyst for improved hydrogen evolution reaction. Renewable Energy, 2019, 143, 1659-1669.	8.9	32
47	Enhanced electrocatalytic properties in MoS2/MoTe2 hybrid heterostructures for dye-sensitized solar cells. Applied Surface Science, 2020, 504, 144401.	6.1	32
48	Application of Plasma-Doping (PLAD) Technique to Reduce Dark Current of CMOS Image Sensors. IEEE Electron Device Letters, 2007, 28, 114-116.	3.9	31
49	Facile synthesis of cobalt–nickel sulfide thin film as a promising counter electrode for triiodide reduction in dye-sensitized solar cells. Energy, 2020, 202, 117730.	8.8	31
50	Dependence of InGaZnO and SnO2 thin film stacking sequence for the resistive switching characteristics of conductive bridge memory devices. Applied Surface Science, 2020, 525, 146390.	6.1	31
51	Intrinsic characteristics of transmission line of graphenes at microwave frequencies. Applied Physics Letters, 2012, 100, .	3.3	30
52	Mixedâ€phase <scp> MoS ₂ </scp> decorated reduced graphene oxide hybrid composites for efficient symmetric supercapacitors. International Journal of Energy Research, 2021, 45, 9193-9209.	4.5	28
53	Highâ€Performance Platinumâ€Free Dyeâ€Sensitized Solar Cells with Molybdenum Disulfide Films as Counter Electrodes. ChemPhysChem, 2015, 16, 3959-3965.	2.1	27
54	Synthesis of MoS _{2(1â^'x)} Se _{2x} and WS _{2(1â^'x)} Se _{2x} alloys for enhanced hydrogen evolution reaction performance. Inorganic Chemistry Frontiers, 2017, 4, 2068-2074.	6.0	27

#	Article	IF	CITATIONS
55	Development of a WS ₂ /MoTe ₂ heterostructure as a counter electrode for the improved performance in dye-sensitized solar cells. Inorganic Chemistry Frontiers, 2018, 5, 3178-3183.	6.0	27
56	Facile and cost-effective growth of MoS2 on 3D porous graphene-coated Ni foam for robust and stable hydrogen evolution reaction. Journal of Alloys and Compounds, 2019, 788, 267-276.	5.5	27
57	Optoelectronics of Multijunction Heterostructures of Transition Metal Dichalcogenides. Nano Letters, 2020, 20, 1934-1943.	9.1	27
58	Self-standing SnS nanosheet array: a bifunctional binder-free thin film catalyst for electrochemical hydrogen generation and wastewater treatment. Dalton Transactions, 2021, 50, 12723-12729.	3.3	27
59	Layer-modulated, wafer scale and continuous ultra-thin WS ₂ films grown by RF sputtering via post-deposition annealing. Journal of Materials Chemistry C, 2016, 4, 7846-7852.	5.5	26
60	Effect of thermal processing on mobility in strained Si/strained Si1â^'yGey on relaxed Si1â^'xGex (x <y) virtual substrates. Applied Physics Letters, 2004, 84, 3319-3321.</y) 	3.3	25
61	Atomic layer deposition of copper nitride film and its application to copper seed layer for electrodeposition. Thin Solid Films, 2014, 556, 434-439.	1.8	25
62	Thicknessâ€Dependent, Gateâ€Tunable Rectification and Highly Sensitive Photovoltaic Behavior of Heterostructured GeSe/WS ₂ p–n Diode. Advanced Materials Interfaces, 2020, 7, 2000893.	3.7	25
63	Study of Grains and Boundaries of Molybdenum Diselenide and Tungsten Diselenide Using Liquid Crystal. Nano Letters, 2017, 17, 1474-1481.	9.1	24
64	WS(1â~'x)Sex Nanoparticles Decorated Three-Dimensional Graphene on Nickel Foam: A Robust and Highly Efficient Electrocatalyst for the Hydrogen Evolution Reaction. Nanomaterials, 2018, 8, 929.	4.1	24
65	A vertical WSe ₂ –MoSe ₂ p–n heterostructure with tunable gate rectification. RSC Advances, 2018, 8, 25514-25518.	3.6	23
66	Designing the MXene/molybdenum diselenide hybrid nanostructures for highâ€performance symmetric supercapacitor and hydrogen evolution applications. International Journal of Energy Research, 2021, 45, 18770-18785.	4.5	23
67	Density functional theory study on the fluorination reactions of silicon and silicon dioxide surfaces using different fluorine-containing molecules. Journal of Vacuum Science and Technology A: Vacuum, Surfaces and Films, 2019, 37, .	2.1	22
68	Theoretical evaluation and experimental investigation of layered 2H/1T-phase MoS2 and its reduced graphene-oxide hybrids for hydrogen evolution reactions. Journal of Alloys and Compounds, 2021, 868, 159272.	5.5	22
69	Impact of Molybdenum Dichalcogenides on the Active and Holeâ€Transport Layers for Perovskite Solar Cells, Xâ€Ray Detectors, and Photodetectors. Small, 2022, 18, e2104216.	10.0	22
70	A highly sensitive enzymeless glucose sensor based on 3D graphene–Cu hybrid electrodes. New Journal of Chemistry, 2015, 39, 7481-7487.	2.8	21
71	A Facile Design of Solution-Phase Based VS2 Multifunctional Electrode for Green Energy Harvesting and Storage. Nanomaterials, 2022, 12, 339.	4.1	21
72	Controlled synthesis and optical properties of polycrystalline molybdenum disulfide atomic layers grown by chemical vapor deposition. Journal of Alloys and Compounds, 2015, 653, 369-378.	5.5	20

#	Article	IF	CITATIONS
73	High Performance MoSe ₂ /Mo Counter Electrodes Based- Dye-Sensitized Solar Cells. Journal of the Electrochemical Society, 2017, 164, E11-E16.	2.9	20
74	Facile Synthesis of Molybdenum Diselenide Layers for High-Performance Hydrogen Evolution Electrocatalysts. ACS Omega, 2018, 3, 5799-5807.	3.5	20
75	MoS2@Mo2C hybrid nanostructures formation as an efficient anode material for lithium-ion batteries. Journal of Materials Research and Technology, 2021, 14, 2382-2393.	5.8	20
76	Fabrication of high-performance graphene field-effect transistor with solution-processed Al2O3 sensing membrane. Applied Physics Letters, 2014, 104, .	3.3	19
77	Ultrathin SiGe Shell Channel p-Type FinFET on Bulk Si for Sub-10-nm Technology Nodes. IEEE Transactions on Electron Devices, 2018, 65, 1290-1297.	3.0	19
78	Twist-Angle-Dependent Optoelectronics in a Few-Layer Transition-Metal Dichalcogenide Heterostructure. ACS Applied Materials & Interfaces, 2019, 11, 2470-2478.	8.0	19
79	Thickness-dependent monochalcogenide GeSe-based CBRAM for memory and artificial electronic synapses. Nano Research, 2022, 15, 2263-2277.	10.4	19
80	Characteristics of Mo2C-CNTs hybrid blended hole transport layer in the perovskite solar cells and X-ray detectors. Journal of Alloys and Compounds, 2021, 885, 161039.	5.5	19
81	Construction of dye-sensitized solar cells using wet chemical route synthesized MoSe2 counter electrode. Journal of Industrial and Engineering Chemistry, 2019, 69, 379-386.	5.8	18
82	Strained-Si–Strained-SiGe Dual-Channel Layer Structure as CMOS Substrate for Single Workfunction Metal-Gate Technology. IEEE Electron Device Letters, 2004, 25, 402-404.	3.9	17
83	Agglomeration effects of thin metal catalyst on graphene film synthesized by chemical vapor deposition. Electronic Materials Letters, 2011, 7, 261-264.	2.2	17
84	Facile preparation of tungsten carbide nanoparticles for an efficient oxalic acid sensor via imprinting. Microchemical Journal, 2020, 159, 105404.	4.5	17
85	Influence of morphological tuned nanostructure hybrid layers on efficient bulk heterojunction organic solar cell and X-ray detector performances. Applied Surface Science, 2021, 543, 148863.	6.1	17
86	RF transmission properties of graphene monolayers with width variation. Physica Status Solidi - Rapid Research Letters, 2012, 6, 19-21.	2.4	16
87	Synthesis of graphene ribbons using selective chemical vapor deposition. Current Applied Physics, 2012, 12, 1113-1117.	2.4	16
88	Atomic layer deposition of cobalt oxide thin films using cyclopentadienylcobalt dicarbonyl and ozone at low temperatures. Journal of Vacuum Science and Technology A: Vacuum, Surfaces and Films, 2013, 31, .	2.1	15
89	Fabrication of InGaZnO-SnO2/PCBM hybrid electron transfer layer for high-performance Perovskite solar cell and X-ray detector. Journal of Alloys and Compounds, 2022, 906, 164399.	5.5	15
90	Morphological evolution, structural and optical investigations of ZnO:Mg (MgxZn1â^'xO (0 ≤ ≤30%)) nanostructures. RSC Advances, 2013, 3, 5465.	3.6	14

#	Article	IF	CITATIONS
91	A progressive route for tailoring electrical transport in MoS2. Nano Research, 2016, 9, 380-391.	10.4	14
92	Selective AuCl3 doping of graphene for reducing contact resistance of graphene devices. Applied Surface Science, 2018, 427, 48-54.	6.1	14
93	Shedding light on the structural, optoelectronic, and thermoelectric properties of pyrochlore oxides (La2Q2O7 (Q = Ge, Sn)) for energy applications: A first-principles investigation. Journal of Solid State Chemistry, 2022, 313, 123305.	2.9	14
94	Hole mobility enhancement in strained-Si/strained-SiGe heterostructure p-MOSFETs fabricated on SiGe-on-insulator (SGOI). Semiconductor Science and Technology, 2004, 19, L48-L51.	2.0	13
95	Fully Depleted Strained-SOI n- and p-MOSFETs on Bonded SGOI Substrates and Study of the SiGe/BOX Interface. IEEE Electron Device Letters, 2004, 25, 147-149.	3.9	13
96	Enhanced performance of graphene by using gold film for transfer and masking process. Current Applied Physics, 2014, 14, 1045-1050.	2.4	13
97	Direct Determination of Field Emission across the Heterojunctions in a ZnO/Graphene Thin-Film Barristor. ACS Applied Materials & amp; Interfaces, 2015, 7, 18300-18305.	8.0	13
98	Study of surface reaction during selective epitaxy growth of silicon by thermodynamic analysis and density functional theory calculation. Journal of Crystal Growth, 2017, 468, 278-282.	1.5	13
99	Development of <scp>MXene</scp> / <scp> WO ₃ </scp> embedded <scp>PEDOT</scp> : <scp>PSS</scp> hole transport layers for highly efficient perovskite solar cells and Xâ€ray detectors. International Journal of Energy Research, 2022, 46, 12485-12497.	4.5	13
100	New Fabrication Technology for Integrating Field Effect Transistors and Diodes. Japanese Journal of Applied Physics, 1996, 35, 1194-1197.	1.5	12
101	Microstructural properties evaluation of SnSSe alloy films. Journal of Materials Science: Materials in Electronics, 2015, 26, 1641-1648.	2.2	12
102	Fabrication of Robust Hydrogen Evolution Reaction Electrocatalyst Using Ag2Se by Vacuum Evaporation. Nanomaterials, 2019, 9, 1460.	4.1	12
103	Eutectoid WxC embedded WS2 nanosheets as a hybrid composite anode for lithium-ion batteries. Ceramics International, 2021, 47, 18646-18655.	4.8	12
104	Tradeoff Between Mobility and Subthreshold Characteristics in Dual-Channel Heterostrucure n- and p-MOSFETs. IEEE Electron Device Letters, 2004, 25, 562-564.	3.9	11
105	Mobility Enhancement in Dual-Channel P-MOSFETs. IEEE Transactions on Electron Devices, 2004, 51, 1424-1431.	3.0	11
106	Cu/MoS ₂ /ITO based hybrid structure for catalysis of hydrazine oxidation. RSC Advances, 2015, 5, 15374-15378.	3.6	11
107	Experimental and theoretical insights to demonstrate the hydrogen evolution activity of layered platinum dichalcogenides electrocatalysts. Journal of Materials Research and Technology, 2021, 12, 385-398.	5.8	11
108	Electrical Characteristics of SiO\$_{2}\$/High-k Dielectric Stacked Tunnel Barriers for Nonvolatile Memory Applications. Journal of the Korean Physical Society, 2009, 55, 116-119.	0.7	11

#	Article	IF	CITATIONS
109	Charge Trapping Characteristics of HfO\$_{2}\$ Layers forTunnel-barrier-engineered Nonvolatile Memory Applications. Journal of the Korean Physical Society, 2009, 55, 962-965.	0.7	11
110	Atomic Layer Deposition of SiO ₂ Thin Films Using Tetrakis(ethylamino)silane and Ozone. Journal of Nanoscience and Nanotechnology, 2012, 12, 3589-3592.	0.9	10
111	Selective growth of graphene in layer-by-layer via chemical vapor deposition. Nanoscale, 2016, 8, 14633-14642.	5.6	10
112	Visualizing Degradation of Black Phosphorus Using Liquid Crystals. Scientific Reports, 2018, 8, 12966.	3.3	10
113	Optimum design for the ballistic diode based on graphene field-effect transistors. Npj 2D Materials and Applications, 2021, 5, .	7.9	10
114	MoO3@MoS2 Core-Shell Structured Hybrid Anode Materials for Lithium-Ion Batteries. Nanomaterials, 2022, 12, 2008.	4.1	10
115	Selfâ€standing <scp>2D</scp> tinâ€sulfideâ€based heterostructured nanosheets: An efficient overall urea oxidation catalyst. International Journal of Energy Research, 2022, 46, 15143-15155.	4.5	10
116	Versatile GeS-based CBRAM with compliance-current-controlled threshold and bipolar resistive switching for electronic synapses. Applied Materials Today, 2022, 29, 101554.	4.3	10
117	Decreasing Dark Current of Complementary Metal Oxide Semiconductor Image Sensors by New Postmetallization Annealing and Ultraviolet Curing. Japanese Journal of Applied Physics, 2008, 47, 139.	1.5	9
118	Low damage-transfer of graphene using epoxy bonding. Electronic Materials Letters, 2013, 9, 517-521.	2.2	9
119	Radio-frequency characteristics of graphene monolayer via nitric acid doping. Carbon, 2014, 78, 532-539.	10.3	9
120	Nearâ€Direct Band Alignment of MoTe ₂ /ReSe ₂ Typeâ€II pâ€n Heterojunction for Efficient VNIR Photodetection. Advanced Materials Technologies, 2022, 7, .	5.8	9
121	Reduction of Random Noise in Complementary Metal Oxide Semiconductor Image Sensors by Gate Oxide Interface Control. Japanese Journal of Applied Physics, 2006, 45, 3466-3469.	1.5	8
122	Ridge Formation and Removal via Annealing in Exfoliated Graphene. Journal of Nanoscience and Nanotechnology, 2011, 11, 5949-5954.	0.9	8
123	Plasma Treatment to Improve Chemical Vapor Deposition-Grown Graphene to Metal Electrode Contact. Japanese Journal of Applied Physics, 2012, 51, 04DN04.	1.5	8
124	Thermoelectric Properties of Ca _{1â^<l>x</l>â^<l>y</l>} Dy _{<l>x</l>} Ce _{<l>y</l>} MnO ₃ for Power Generation. Journal of Nanoscience and Nanotechnology, 2011, 11, 7176-7179.	0.9	7
125	Effects of hydrogen in the cooling step of chemical vapor deposition of graphene. Electronic Materials Letters, 2013, 9, 417-420.	2.2	7
126	Schottky barrier height modulation and photoconductivity in a vertical graphene/ReSe2 vdW p-n heterojunction barristor. Journal of Materials Research and Technology, 2022, 17, 2796-2806.	5.8	7

#	Article	IF	CITATIONS
127	Fabrication of High-Performance Solar Cells and X-ray Detectors Using MoX ₂ @CNT Nanocomposite-Tuned Perovskite Layers. ACS Applied Materials & Interfaces, 2022, 14, 33626-33640.	8.0	7
128	Dedicated Process Architecture and the Characteristics of 1.4 Å; m Pixel CMOS Image Sensor with 8M Density. , 2007, , .		6
129	Fabrication of Low Temperature Polycrystalline Silicon Thin-Film Transistor Nonvolatile Memory Devices for Digital Memory on Glass Applications. Japanese Journal of Applied Physics, 2008, 47, 2728-2732.	1.5	6
130	Graphene film growth on sputtered thin Cu–Ni alloy film by inductively coupled plasma chemical vapor deposition. RSC Advances, 2014, 4, 63349-63353.	3.6	6
131	Comparison studies on electrodeposited CdSe, SnSe and Cd x Sn1â^'x Se thin films. Ionics, 2015, 21, 1187-1192.	2.4	6
132	Hierarchical Mo2C@CNT Hybrid Structure Formation for the Improved Lithium-Ion Battery Storage Performance. Nanomaterials, 2021, 11, 2195.	4.1	6
133	Dependence of Subthreshold Hump and Reverse Narrow Channel Effect on the Gate Length by Suppression of Transient Enhanced Diffusion at Trench Isolation Edge. Japanese Journal of Applied Physics, 2000, 39, 2136-2140.	1.5	5
134	Dynamics of liquid crystal on hexagonal lattice. 2D Materials, 2018, 5, 045021.	4.4	5
135	Density functional theory study on the modification of silicon nitride surface by fluorine-containing molecules. Applied Surface Science, 2021, 554, 149481.	6.1	5
136	Fullerene-free, MoTe2 atomic layer blended bulk heterojunctions for improved organic solar cell and photodetector performance. Journal of Materials Research and Technology, 2022, 17, 2875-2887.	5.8	5
137	Sensitive Strain Measurements of Bonded SOI Films Using MoirÉ. IEEE Transactions on Semiconductor Manufacturing, 2004, 17, 35-41.	1.7	4
138	Charge Trapping Characteristics of Variable Oxide Thickness Tunnel Barrier with SiO2/HfO2or Al2O3/HfO2Stacks for Nonvolatile Memories. Japanese Journal of Applied Physics, 2009, 48, 06FD11.	1.5	4
139	Hole mobility and device characteristics of SiGe dual channel structure. Current Applied Physics, 2009, 9, S47-S50.	2.4	4
140	Effects of alloying 30 at. % Ni using a Cu catalyst on the growth of bilayer graphene. Electronic Materials Letters, 2012, 8, 609-616.	2.2	4
141	Visibility of hexagonal boron nitride on transparent substrates. Nanotechnology, 2020, 31, 195701.	2.6	4
142	Plasma Treatment to Improve Chemical Vapor Deposition-Grown Graphene to Metal Electrode Contact. Japanese Journal of Applied Physics, 2012, 51, 04DN04.	1.5	4
143	Decoration of X2C nanoparticles on CdS nanostructures for highly efficient photocatalytic wastewater treatment under visible light. Applied Surface Science, 2022, 583, 152533.	6.1	4
144	Novel Dual Gate Oxide Process with Improved Gate Oxide Integrity Reliability. Electrochemical and Solid-State Letters, 1999, 3, 56.	2.2	3

#	Article	IF	CITATIONS
145	Two-step rapid thermal annealing (TS-RTA) to suppress out-diffusion of dopants without degrading short channel effect of transistor. IEEE Electron Device Letters, 2000, 21, 376-377.	3.9	3
146	Characteristics of Schottky-barrier source/drain metal-oxide-polycrystalline thin-film transistors on glass substrates. Journal of the Korean Physical Society, 2012, 60, 6-9.	0.7	3
147	Raman spectroscopic image analysis on micropatterned graphene. Micro and Nano Letters, 2013, 8, 362-365.	1.3	3
148	Highly Fast Response of Pd/Ta2O5/SiC and Pd/Ta2O5/Si Schottky Diode-Based Hydrogen Sensors. Sensors, 2021, 21, 1042.	3.8	3
149	1/2.5" 8 mega-pixel CMOS Image Sensor with enhanced image quality for DSC application. , 2006, , .		2
150	High frequency transmission properties of graphene monolayer with different coplanar waveguide electrode configurations. , 2011, , .		2
151	Fast and simultaneous growth of graphene, intermetallic compounds, and silicate on Cu–Ni alloy foils. Materials Chemistry and Physics, 2014, 147, 452-460.	4.0	2
152	Capacitance behavior of radio-frequency interdigital capacitor with single- and multi-layer graphenes. Applied Physics Letters, 2017, 110, .	3.3	2
153	Process Steps for High Quality Si-Based Epitaxial Growth at Low Temperature via RPCVD. Materials, 2021, 14, 3733.	2.9	2
154	Highly Active Mo2C@WS2 Hybrid Electrode for Enhanced Hydrogen Evolution Reaction. Catalysts, 2021, 11, 1060.	3.5	2
155	Rectifying Effect in a High-Performance Ballistic Diode Bridge Based on Encapsulated Graphene with a Unique Design. ACS Applied Electronic Materials, 2022, 4, 1518-1524.	4.3	2
156	Electrical properties of organic field effect transistors with thin graphite/metal electrode directly grown by ICP-CVD at low temperatures. Current Applied Physics, 2013, 13, 1275-1279.	2.4	1
157	Siâ€core/SiGeâ€shell channel nanowire FET for subâ€10â€nm logic technology in the THz regime. ETRI Journal, 2019, 41, 829-837.	2.0	1
158	Deep-Ultraviolet (DUV)-Induced Doping in Single Channel Graphene for Pn-Junction. Nanomaterials, 2021, 11, 3003.	4.1	1
159	Study of Optimization Guidelines on Nitrogen Concentration in Nitrided Oxide for Logic and Dynamic Random Access Memory Application. Japanese Journal of Applied Physics, 2000, 39, 2203-2207.	1.5	0
160	SiGe Heterojunction FinFET Towards Tera-Hertz Applications. Journal of the Korean Physical Society, 2018, 72, 527-532.	0.7	0
161	Three-Dimensional stacked CMOS Inverters Using Laser-Crystallized Poly-Si TFTs. Journal of the Korean Physical Society, 2009, 54, 1798-1801.	0.7	0
162	Purity Evaluation of Single-Walled Carbon Nanotubes Using Thermogravimetric Analysis. Journal of Korean Institute of Metals and Materials, 2013, 51, 137-144.	1.0	0